Biomedicine & Pharmacotherapy 133 (2021) 110954

Contents lists available at ScienceDirect

Biomedicine & Pharmacotherapy

journal homepage: www.elsevier.com/locate/biopha

Original article

Anemarrhena asphodeloides modulates gut microbiota and restores pancreatic function in diabetic rats

Dong Yan [a,b,1], Pengcheng Fan [c,1], Wenlong Sun [d,1], Qianzhi Ding [a,1], Wei Zheng [a], Weidi Xiao [c], Bowei Zhang [d], Tao Zhang [b], Tao Zhang [c], Jiahui Shi [c,e], Xiaojuan Chen [a], Peiru Chen [c,e], Jie Zhang [a], Ying Hao [f], Xinguang Sun [a], Xu Pang [a], Yuesheng Dong [d,****], Ping Xu [c,e,***], Liyan Yu [b,**], Baiping Ma [a,*,2]

[a] Beijing Institute of Radiation Medicine, Beijing, China
[b] China Pharmaceutical Culture Collection, Institute of Medicinal Biotechnology, Chinese Academy of Medical Sciences & Peking Union Medical College, Beijing, China
[c] State Key Laboratory of Proteomics, Beijing Proteome Research Center, National Center for Protein Sciences, Institute of Lifeomics, Beijing, China
[d] School of Bioengineering, Dalian University of Technology, Dalian, China
[e] Hebei Province Key Lab of Research and Application on Microbial Diversity, College of Life Sciences, Hebei University, Baoding, China
[f] School of Life Sciences, Beijing University of Chinese Medicine, Beijing, China

ARTICLE INFO

Keywords:
Anemarrhena asphodeloides
Gut microbiota
Blautia
Peroxiredoxin 4
Diabetes

ABSTRACT

Anemarrhena asphodeloides is an herb widely used to treat symptoms associated with diabetes in traditional Chinese medicine. However, its key components and metabolites have low bioavailability and poor host absorption. To clarify the anti-diabetic mechanism of *A. asphodeloides* extract (AAE), we examined the anti-diabetic effects of AAE in rats with diabetes induced by a high-fat diet and streptozotocin. Faeces levels of the main components and metabolites of AAE were significantly higher than levels in plasma, which indicated that gut microbiota might play important roles in its anti-diabetic effect. Microbiological studies showed that unabsorbed components increased the diversity of the gut microbiota, enriched potentially beneficial bacteria, and suppressed potentially harmful bacteria. *In vitro* studies showed that AAE promoted the proliferation of *Blautia coccoides*, a bacterium with positive implication for diabetes, in a dose-dependent manner. AAE also promoted pancreatic cell regeneration and restored the function of pancreatic islet cells *via* peroxiredoxin 4 overexpression. Overall, these results suggest that AAE alleviates diabetes *via* modulating gut microbiota and protein expression.

1. Introduction

Type 2 diabetes mellitus is a progressive metabolic disease spreading worldwide. Over 425 million people suffer from diabetes, approximately 90 % of the people diagnosed with diabetes are type 2 diabetics [1]. Diabetes mellitus is characterized by high blood glucose levels, plasma lipid abnormalities, high insulin resistance, and pancreatic β-cell dysfunction [2,3]. If the blood glucose is out of control, the patients would suffer many diabetic complications, including neuropathy and vasculopathy. The mainstay of diabetes treatment used to be blood glucose control in order to prevent the development of complications.

There is increasing evidence to suggest that the gut microbiota plays a role in the development of diabetes [4–9]. Several studies have demonstrated the involvement of the gut microbiota in insulin signalling [10], glucose homeostasis [11], and low-grade inflammation [12,13]. In addition, there are some traditional Chinese medicines (TCMs) with low oral bioavailability that have effects on diabetic treatment [14]. The TCMs with low oral bioavailability mainly distributed in the gut, which

* Corresponding author at: Beijing Institute of Radiation Medicine, 27 Taiping Road, Haidian District, Beijing, 100850, China.
** Corresponding author at: China Pharmaceutical Culture Collection, Institute of Medicinal Biotechnology, Chinese Academy of Medical Sciences & Peking Union Medical College, 1 Tian Tan Xi Li, Dongcheng District, Beijing, 100050, China.
*** Corresponding author at: Beijing Proteome Research Center, 38 Science Park Road, Changping District, Beijing, 102206, China.
**** Corresponding author at: School of Bioengineering, Dalian University of Technology, 2 Linggong Road, Dalian, 116024, China.
E-mail addresses: yshdong@dlut.edu.cn (Y. Dong), xuping_bprc@126.com (P. Xu), yly@cpcc.ac.cn (L. Yu), mabaiping@sina.com (B. Ma).
[1] These authors contributed equally to this work.
[2] Lead contact.

https://doi.org/10.1016/j.biopha.2020.110954
Received 23 August 2020; Received in revised form 23 October 2020; Accepted 27 October 2020
Available online 29 November 2020

may alleviate diabetes through the gut microbiota [6,9]. Therefore, gut microbiota can provide a new perspective for understanding the mechanisms of low-bioavailable natural products.

Anemarrhena asphodeloides is one of the most commonly used component herbs in TCM products currently approved for diabetes treatment in China [14,15]. *A. asphodeloides* extract (AAE) and its main components have shown anti-diabetic effects [16]. However, the main components of AAE, comprising mostly flavonoids and saponins, have low oral bioavailability in the body [17,18]. The mangiferin, one of the main flavonoids in AAE, showed its poor oral bioavailability [19] and hypoglycemic activity with increasing pyruvate oxidation and ATP production [20]. The timosaponin BII, one of the main saponins in AAE, had protect effect on pancreatic β cells by decreasing IL-1β production and low oral bioavailability (1.1 %) on rat [21]. TongGuanWan, a TCM formula product which contains mangiferin, timosaponin BII, and timosaponin AIII as main constituents, could lower blood glucose and improve glucose tolerance in *db/db* mice [22]. Previous studies indicated an apparent contradiction between the low oral bioavailability and anti-diabetic effects of AAE [23–25], prompting us to investigate the modulation of gut microbiota in this phenotype. In the current study, the main goal was to clarify the mechanisms of AAE on diabetic rats induced with high-fat diet and streptozotocin, and to propose potential strategy for diabetes treatment.

2. Materials and methods

2.1. Preparation of AAE

The dried rhizomes of *A. asphodeloides* (2.5 kg, voucher No. 20,007,751), which were collected from Anguo, Hebei province, China, were cut into small pieces and extracted three times with distilled water (20 L each) at 120 ℃ (each time for 1 h). The crude extract was concentrated under vacuum to a small volume (0.33 g mL^{-1}), and ethanol was then added to 30 % to remove macromolecular substances. After standing for 24 h, the supernatant was collected, concentrated under vacuum, and freeze-dried to obtain the AAE. The extraction yield of *A. asphodeloides* rhizomes was 40 %.

2.2. Qualitative analysis of AAE by ultra-high performance liquid chromatography coupled with hybrid quadrupole time-of-flight mass spectrometry (UPLC–Q–TOF/MS)

Chromatographic separation was performed using an Acquity UPLC system (Waters, MA, USA) equipped with an HSS T3 column (100 mm × 2.1 mm, 1.8 μm). AAE (5 mg) was dissolved with 70 % ACN (4 mg mL^{-1}), and 1 μL of this mixture was then injected into the column and eluted with the mobile phase at 0.6 mL min^{-1} and 45 °C. Mobile phases A and B consisted of 0.1 % FA solution and ACN containing 0.1 % FA, respectively. The gradient program was as follows: 0–0.1 min, 5% B; 0.1–5 min, 5%–10 % B; 5–8 min, 10 %–15 % B; 8–9 min, 15 %–20 % B; 9–11 min, 20 %–22 % B; 11–13 min, 22 % B; 13–19 min, 22 %–38 % B; 19–24 min, 38 %–50 % B; 24–28.5 min, 50 %–65 % B; 28.5–33.5 min, 65 %–85 % B; 33.5–35 min, 85 %–90 % B; and 35–36 min, 90 %–95 % B. The eluent was introduced into a SYNAPT G1-Si high-definition mass spectrometer (Waters) equipped with an electrospray ionization (ESI) source. Analyses were performed in both positive- and negative-ion modes. The sampling cone and capillary voltages were 40.0 V and 3000 V, respectively; the source temperature was 100 °C, and the desolvation gas flow and temperature were 850 L h^{-1} and 450 °C, respectively. Data were collected in centroid mode from 100 to 1500 Da in full scan over 0–36 min. Leucine enkephaline was used as lock mass in both positive- ($[M+H]^+$ = 556.2771) and negative-ion modes ($[M-H]^-$ = 554.2615) *via* a lock spray interface at a flow-rate of 50 μL min^{-1} to ensure accuracy during the MS analysis. The instrument was controlled by Masslynx 4.1 software (**Fig. S1** and **Table S1**).

2.3. Animals, pancreas tissue, serum, and faecal samples

Male SPF Wistar rats (8 weeks old, 160–200 g) were purchased from the SPF Laboratory Animal Centre, Dalian Medical University, with permission number SCXK 2013–0003. All animals were maintained under standard laboratory conditions and placed in a suitable SPF environment under a 12-h day/night alternating cycle according to the Guide for the Care and Use of Laboratory Animals (NIH). Eighty rats were fed a high-fat diet (HFD, D12450) for 3 weeks. Then, the mice fed HFD were injected intraperitoneally with 40 mg/kg STZ and then OGTTs were tested on the 7th and 21 st days after injection. Only rats that met the standard for diabetes (level of 2 h-postprandial glucose > 11.1 mM in both OGTTs) were selected as type 2 diabetic rat models (n = 30). Other rats fed a normal diet were used as negative controls (n = 6). All rats had free access to water. The OGTT was conducted by oral administration of 2 g kg^{-1} glucose after 16 h fasting. Blood samples were then collected from the tail vein and blood glucose levels were measured three times at 0 and 120 min, using the glucose oxidase method [26]. Type 2 diabetic model rats induced by HFD and streptozotocin were divided into four groups (n = 5 or 6), randomized with respect to bodyweight, fasting blood glucose (FBG), and 2 h-postprandial glucose (2h-PG). The groups were orally administered placebo (5% CMC-Na; DM group), 20 mg kg^{-1} day^{-1} AAE (LD group), 60 mg kg^{-1} day^{-1} AAE (MD group), or 180 mg kg^{-1} day^{-1} AAE (HD group), respectively, by gavage for 4 weeks. OGTTs were performed, bodyweights were measured, and stool samples were collected at week 0, 2, and 4 used a commercial excrement collector (Majorbio Bio-Pharm Technology Co. Ltd. Shanghai, China).

Blood samples were collected and centrifuged at 4000 ×g for 5 min at 4 °C to obtain plasma. Lipopolysaccharide (LPS), tumour necrosis factor-α (TNFα), total cholesterol (TC), triglycerides (TG), and fasting insulin level in the plasma were measured using commercially available kits (Jiancheng Co. Ltd, Nanjing, China). For tissue studies, liver and ileum were excised from the rats and stored in liquid nitrogen for lipid profiles (TC and TG) or TNFα analysis. For histological studies, pancreas tissue and liver were excised from the rats, collected, and stored in 10 % formalin.

All reagents used, including acetonitrile (ACN; Fisher Scientific Co. Ltd, Loughborough, UK), formic acid (FA; DikmaPure Scientific Co. Ltd, Beijing, China), dimethyl sulfoxide (Tedia Company Inc., Ohio, USA), and methanol (Sigma-Aldrich, St. Louis, MO, USA), were of chromatographic purity. Distilled water was purified by Lab Tower EDI 15 (Thermo-Fisher Scientific, MA, USA).

2.4. Quantitative analysis of faecal and plasma samples by UPLC triple quadrupole MS

To know more about the distribution of key components, a quantitative study was carried on faecal and plasma samples. The structures of seven previously isolated chemical standards (neomangiferin, mangiferin, norathyriol, sarsasapogenin, timosaponin BII, B, and AIII) were confirmed by MS and nuclear magnetic resonance spectroscopy [27]. Linezolid (Batch No. 20,160,301; purity > 99.5 %; Sichuan Saizhuo Pharmacy Co. Ltd, Mianyang, China) was used as an internal standard.

Faeces were homogenized in nine volumes of distilled water, and 50 μL of the faecal homogenates and plasma samples were individually mixed with 150 μL ACN. All samples were vortexed for 1 min, centrifuged for 15 min at 4415 × *g* and 4 °C, and 50 μL of supernatant was then collected from each sample, mixed with 50 μL distilled water, and 2 μL of mixture was injected into the liquid chromatography-tandem mass spectrometry (LC–MS/MS) for analysis. The API 6500 triple quadrupole mass spectrometer, Turbo Ion Spray ESI source, and Analyst 1.6.2 data processing system were purchased from AB Sciex (Framingham, MA, USA). The HPLC system was purchased from Shimadzu Corporation (Japan).

Separations were carried out in a Kinetex C18 (3.0 mm × 50 mm, 2.6

μm) column at a flow rate of 0.8 mL min^{-1}. Mobile phases A and B consisted of 0.1 % FA solution and ACN containing 0.1 % FA, respectively. The gradient elution was carried out as follows: 0–0.5 min, 2% B; 0.5–3.5 min, 2%–95 % B; 3.5–4 min, 95 % B. ACN/water (9:1, v/v) was chosen as the needle rinse solution. The volume of injection was 2 μL and the auto-sampler was maintained at room temperature.

The mass spectrometer detector was set for multiple reaction monitoring (MRM) in both positive- and negative-ion modes. The MRM transitions and correlative parameters were as follows: ion spray voltage, 5.5 kV in ESI^+ and 4.5 kV in ESI^-; collision gas, 12 psi; curtain gas, ESI^+, 30 psi; ESI^-, 20 psi; ion source gas 1, 50 psi, ion source gas 2, 50 psi; and source temperature, 550 °C. Detection was performed using both positive- and negative-ion ESI in MRM modes (**Table S2**).

2.5. DNA extraction and polymerase chain reaction (PCR) amplification

Genomic DNA was extracted from each stool sample using a QIAamp Fast DNA Stool Mini Kit (Qiagen, Germany) according to the manufacturer's protocols. The V3–V4 region of the bacterial rRNA gene was amplified by PCR (95 °C for 3 min, followed by 27 cycles comprising 95 °C for 30 s, 55 °C for 40 s and 72 °C for 45 s, and ended by 72 °C for 10 min) using primers 338 F (5′-barcode-ACTCCTACGGGAGGCAGCA-3′) and 806R (5′-GGACTACHVGGGTWTCTAAT-3′) [28], where the barcode was an eight-base sequence unique to each sample. The PCR amplification was conducted using high-fidelity TransStart Fastpfu DNA Polymerase (Transgen, China). PCR reactions were performed in triplicate using individual 20 μL mixtures containing 4 μL of 5 × FastPfu Buffer, 2 μL of 2.5 mM dNTPs, 0.8 μL of each primer (5 μM), 0.4 μL of FastPfu Polymerase, and 10 ng of template DNA.

2.6. Illumina MiSeq sequencing

Amplicons were purified using an AxyPrep DNA Gel Extraction Kit (Axygen, CA, USA) according to the manufacturer's instructions, and quantified using QuantiFluor™-ST (Promega, WI, USA). Purified amplicons were pooled in equimolar ratios and paired-end sequenced (2 × 250 bp) on an Illumina MiSeq platform, according to the manufacturer's protocol.

2.7. DNA sequencing data analysis

Raw files were demultiplexed and quality-filtered using QIIME (version 1.9.0) [29] with the following criteria: (1) 300 bp reads with an average quality score < 20 over a 50 bp sliding window were truncated, and truncated reads < 50 bp were discarded; (2) reads with two nucleotide mismatches in primer matching and reads containing ambiguous characters were both removed; and (3) only sequences with overlap > 10 bp were assembled. Reads that could not be assembled were discarded.

All samples were subsampled at the same sequence depth (22,574 reads). Operational taxonomic units (OTUs) were clustered with 97 % similarity cut-off using UPARSE (version 7.1, http://drive5.com/uparse/). Chimeric sequences were identified and removed using UCHIME. OTUs were used as the basis for calculating α and β diversity metrics. The taxonomy of each 16S rRNA gene sequence was analysed by RDP Classifier [30] against the SILVA (SSU115) 16S rRNA database using a confidence threshold of 70 % [31]. The OTU diversity was analysed using Chao1. Good's coverage estimator and Shannon's index were calculated using QIIME 1.9.0 software [29]. Analysis of similarities (ANOSIM) was performed using QIIME 1.9.0 software to detect significantly different bacterial community compositions among the groups.

2.8. SCFA quantification by GC–MS

Faecal SCFAs were quantified as described previously [32]. A volume of 1000 μL of 0.005 M NaOH solution containing isocaproic acid (5 μg mL^{-1} isocaproic acid) was added to 150 mg faecal samples, homogenized for 10 min, and then centrifuged at 13,200 × *g* and 4 °C for 20 min. A volume of 475 μL supernatant of faecal water was transferred into a 2 mL glass centrifuge tube and 25 μL of phosphoric acid was added.

Analysis was performed using an Agilent 7890A GC system coupled to a Flamed ionization detector (Agilent Technologies, CA, USA). SCFAs were separated using a polar DB-FFAP capillary column (30 m × 0.25 mm internal diameter, 0.25 μm film thickness; Agilent). One microliter of derivative was injected in split mode at a ratio of 20:1 at a constant flow rate of 1 mL min^{-1}. Nitrogen was used as the carrier gas. The oven was initially set at 60 °C for 5 min, increased to 250 °C at a rate of 10 °C min^{-1}, and maintained at 250 °C for 5 min. The temperatures of the front inlet, transfer line, and electron impact ion source were set at 280, 250, and 230 °C, respectively.

2.9. Faecal incubation with AAE in vitro

To confirm the interaction between the gut microbiota and AAE *in vitro*, we sequenced DM faecal samples after incubation with AAE. Faeces from DM rats were collected at week 0 and incubated using a Bug Box Plus anaerobic workstation (Ruskinn Technology Ltd, Bridgend, UK). Faeces (0.3 g) were then diluted in three volumes of saline (1.2 mL), followed by the addition of 0 (eDM group, which means DM group in *ex vivo* experiment), 10.24 (eMD group, which means medium-dose of AAE in *ex vivo* experiment and is similar to the exposure concentration of AAE in the MD group), and 30.72 mg mL^{-1}(eHD group, which means high-dose of AAE in *ex vivo* experiment and is similar to the exposure concentration of AAE in the HD group) AAE to the samples, respectively. Three-quarters of each sample were cultured under anaerobic conditions at 37 °C for 0, 8, 24, and 48 h, while the remaining quarter was stored at −20 °C. Amplicon sequencing was performed using an Illumina MiSeq platform. Faecal SCFAs were quantified by GC—MS.

2.10. Blautia coccoides (JCM 1395 ^{T}) incubation with AAE in vitro

To verify the anti-diabetic mechanism of AAE through gut microbiota, a commercially available strain of *B. coccoides* was cultured in liquid medium containing varying levels of AAE for 24 h. *B. coccoides* (JCM 1395^T) was purchased from the Japan Collection of Microorganisms. The strain was cultured in liquid medium under anaerobic conditions with AAE at concentrations of 0, 32, 256, 512, 1024, and 2048 μg mL^{-1} for 24 h. The OD_{600nm} was measured using a Bioscreen C MBR machine (Oy Growth Curves Ab Ltd, Helsinki, Finland).

2.11. Protein extraction and gel-assisted digestion

Rat pancreas tissue was freeze-dried in liquid nitrogen using a pestle and mortar. The powder was added to lysis buffer comprising 9 M urea, 10 mM iodoacetamide, 100 mM NH_4HCO_3 and 1 × protein inhibitor cocktail (Sigma-Aldrich Ltd, Oakville, Canada), sonicated, and centrifuged for 2 min at 17,000 × *g* and 4 °C. The supernatant was collected and the protein concentration was measured by bicinchoninic acid assay. Protein separation was performed by short SDS-PAGE stained with Coomassie Blue G-250 [33]. Pancreas proteome samples (~100 μg) were reduced, alkylated, and digested with 10 ng μL^{-1} trypsin for 12 h at 37 °C as described previously [33].

2.12. Tandem mass tag (TMT) labelling

TMT chemical derivatization labelling with different channels of the same isobaric tag leads to molecules with very similar or identical mass that appear as a single peak in full MS scans and can be isolated in subsequent MS/MS analysis. Quantification is based on the relative intensities of reporter ions which appear in the low mass range of MS/MS spectra [34]. Peptides from the different cell groups were labelled using six-plex TMT, according to the manufacturer's instructions (Thermo

Fisher Scientific Ltd, Carlsbad, CA, USA) [35]. Peptides from the control, DM, LD, MD, and HD groups were labelled with 126, 127 N, 128 N, 128C, and 129 N tags, respectively. To ensure high-accuracy quantitation, the tag peptide ratio was selected as 126:127 N:128 N:128C:129 N = 1:1:1:1:1. The labelled peptides were then pooled and separated into 12 fractions by high-pH reverse-phase high performance liquid chromatography, followed by nanoAcquity UPLC–MS/MS analysis with a Lumos mass spectrometer. Technical LC—MS/MS variations were detected by repeated analysis of the same TMT labelling samples to identify the true biological relevance of the results.

2.13. Data processing and database searching

All raw files were submitted to the Protein discovery software (version 1.6.0.1, Martinsried, Germany) and compared against the UniProt rat protein database (version June 2017). The target-decoy based strategy was used to achieve a peptide and protein false discovery rate (FDR) ≤ 1%. The search parameters were as described previously [33]. Gene Ontology annotation was performed using DAVID [36]. Pathway and protein–protein interaction analyses were performed using the Kyoto Encyclopedia of Genes and Genomes [37,38] and STRING [39], respectively.

2.14. Histological and immunofluorescence studies

For histological analyses, tissue samples were fixed in formalin solution for 24 h and then embedded in paraffin. For immunofluorescence analyses, pancreas sections were cut at 3 μm thick and stained with HE. Some were incubated with antibodies against insulin (Boster Biological Technology Co. Ltd, Wuhan, China) and glucagon (Beijing Biosynthesis Biotechnology Co. Ltd, Beijing, China) at a ratio 1:100 overnight at 4 °C. PRDX4 immunofluorescence studies were performed using anti-

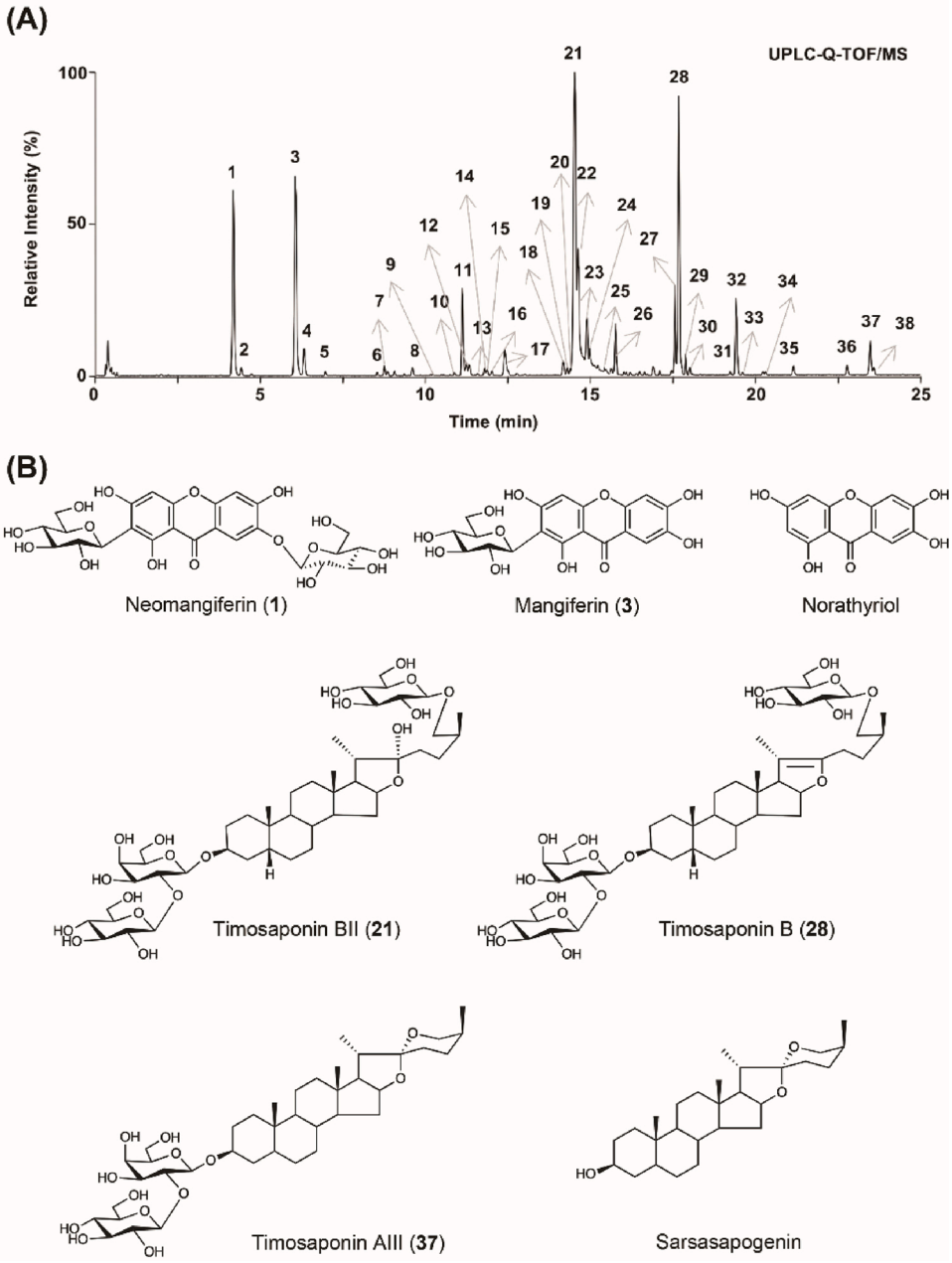

Fig. 1. (**A**) Base peak ion chromatogram of *Anemarrhena asphodeloides* extract (AAE) profiled by UPLC-Q-TOF/MS, characterizing eight flavonoids and 30 steroidal saponins. (**B**) Structures of main abundant compounds identified in AAE.

peroxiredoxin 4 antibody (ab59542, Abcam Co. Ltd, Cambridge, MA, USA). Other sections were incubated with goat anti-rabbit (fluorescein isothiocyanate) and goat anti-mouse (tetramethylrhodamine) antibodies at a ratio of 1:200 for 1 h at 4 °C. All incubated samples were washed three times with 0.05 mmol L^{-1} Tris−HCl (pH = 7.4). Stained samples were observed under a fluorescence microscope at 100× and 400× magnifications.

2.15. Statistical analysis

Statistical analysis was performed using Statistical Package for the Social Sciences (SPSS, version 17.0). Comparisons between groups were analysed by one-way analysis of variance (ANOVA) followed by Tukey's multiple comparison. A value of $p < 0.05$ was considered to be statistically significant. The canonical correspondence analysis (CCA) and principal co-ordinates analysis (PCoA) were conducted using R software (version 3.7.0) with the vegan package [40]. Heatmaps and Venn diagrams were plotted using R software (version 3.7.0) and bar and line graphs were plotted using Origin software (version 8.0). Post-hoc tests for ANOVA were performed using Statistical Analysis of Metagenomics Profiles software (STAMP) [41] to identify significantly different genera between MD and DM rats.

3. Results

3.1. AAE improved blood glucose levels, lipid profiles, and inflammation

The chemical composition of AAE was profiled using UPLC-QTOF/MS (Fig. 1A). Based on the exact mass, fragment ions, retention times, the published literatures, and compared with the standards, eight flavonoids and 30 saponins were detected (Table S**1**) in the base peak ion chromatogram.

The FPG and 2h-PG levels were significantly higher in DM group compared with NM group and the 2h-PG levels were significantly reduced in the MD and HD groups with DM group, while the FPG levels in the LD, MD, and HD groups were no significant difference with DM

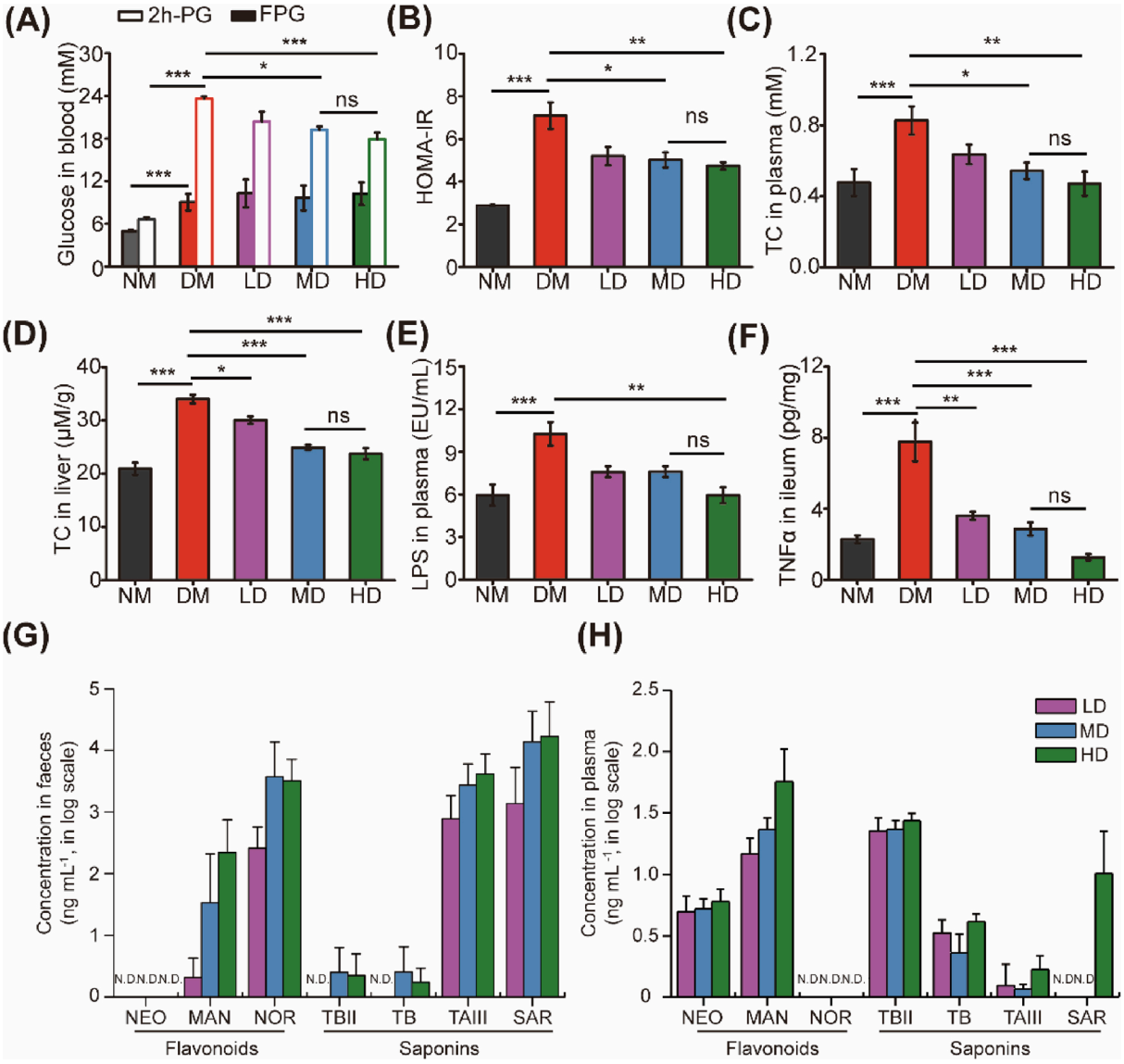

Fig. 2. AAE improved blood glucose and lipid profiles. (**A**) Blood glucose levels at week 4; (**B**) HOMA-IR; (**C**) TC in plasma; (**D**) TC in liver; (*E*) LPS in plasma; (**F**) TNFα in ileum. Values shown as mean ± standard error (SEM). $^{*}p < 0.05$, $^{**}p < 0.01$, $^{***}p < 0.001$ by one-way analysis of variance (ANOVA) followed by Tukey's multiple comparison, NS means no significant differences detected. Metabolite contents (log scale) of rat faeces (**G**) and plasma (**H**) in the fourth week after administration. Values in (**G**) and (**H**) are shown as mean ± SEM (log scale). N.D. means not detected. NEO: neomangiferin; MAN: mangiferin; NOR: norathyriol; TBII: timosaponin BII; TB: timosaponin B; TAIII: timosaponin AIII; SAR: sarsasapogenin.

group (Fig. 2A). Compared with DM group, the insulin level and homeostasis model assessment of insulin resistance (HOMA-IR) index were also significantly decreased in the MD and HD groups (Fig. 2**B** and **Fig. S1A**). Notably, rats in the HD group were significantly reduced levels of TC in plasma and liver, LPS in plasma, and TNFα in the ileum, compared with DM rats (Fig. 2**C–F**, Fig. S**1B** and **C**). Interestingly, there were no significant differences in bodyweight among the groups during AAE treatment (Fig. S**1D** and **E**), and no differences in plasma or liver TNFα levels (Fig. S**1F** and **G**).

We performed a quantitative study to identify the key components and metabolites of AAE in faeces and plasma. AAE was previously shown to contain various flavonoids and saponins, including neomangiferin, mangiferin, norathyriol, timosaponin BII, timosaponin B, timosaponin AIII, and sarsasapogenin (Fig. 1**B**) [42–45]. We analysed faecal and plasma samples using LC–MS/MS and identified these compounds in rats that had undergone AAE treatment (Fig. 2**G** and **H**). Specifically, mangiferin, norathyriol, timosaponin BII, timosaponin B, timosaponin AIII, and sarsasapogenin were detected in faecal samples, while neomangiferin, mangiferin, timosaponin BII, timosaponin B, timosaponin AIII, and sarsasapogenin were detected in plasma samples. The neomangiferin was only detected in plasma while the norathyriol was only detected in faeces. The concentrations of the main metabolites in faeces were generally significantly (several orders) higher than in plasma samples. The detailed data are shown in **Table S2**.

3.2. AAE affected the diversity and composition of the gut microbiota in vivo and in vitro

Growing evidence suggests that the gut microbiota is involved in diabetes progression [4,6,9]. We examined the effects of AAE on the diversity and composition of the gut microbiota by sequencing faecal samples taken at week 0, 2, and 4. A total of 4,407,100 valid reads were obtained (**Table S3**). Rarefaction curves based on observed OTUs and Shannon indices indicated that the dominant phylotypes were captured (**Fig. S2A** and **B**). Interestingly, the MD group had the highest Shannon index at all time points (Fig. 3**A** and **B**). Furthermore, a Venn diagram showed that the number of unique OTUs at week 4 was highest in the MD group and lowest in the DM group (**Fig. S2C–E**). These results suggest that there was an optimal dose of AAE for improving the diversity of the gut microbiota.

PCoA showed that the composition of the bacterial community differed significantly between the MD and DM groups (Fig. 3**C–E** and **Fig. S2F**). Community-composition analysis showed changes in bacterial phyla and genera at 4 weeks after AAE treatment (**Table S4** and **S5; Fig. S3A** and **B**). Specifically, the abundance of the phylum Proteobacteria was decreased in the MD and HD groups, whereas Bacteroidetes and Actinobacteria were increased. Heatmap analysis showed increased abundances of the genera *Blautia*, *Roseburia*, *Phascolarctobacterium,* and *Enterococcus* in the MD group, but decreased abundances of *Brachyspira*, *Facklamia*, *Klebsiella*, *Oligella*, and *Escherichia-Shigella* at week 4 (Fig. 3F).

To examine the interaction between the gut microbiota and AAE, we sequenced DM faecal samples after incubation with AAE 10.24 mg mL^{-1} (eMD group, which means medium-dose of AAE in *ex vivo* experiment and is similar to the exposure concentration of AAE in the MD group), 30.72 mg mL^{-1} (eHD group, which means high-dose of AAE in *ex vivo* experiment and is similar to the exposure concentration of AAE in the HD group), and 0 mg mL^{-1} (eDM group, which means DM group in *ex vivo* experiment) for 0, 8, 24, and 48 h. A total of 36 incubation samples were sequenced and 4,124,202 valid reads were observed (**Table S3, Fig. S4A** and **B**). The diversity was particularly increased in the eMD group. This result was consistent with that observed *in vivo* (**Fig. S4C**). A Venn diagram showed that the number of unique OTUs after 48 h incubation was highest in the eMD group (**Fig. S4D–F**). Furthermore, the gut microbiota community composition differed significantly between the eMD and eNM groups after 48 h incubation (ANOSIM, $p < 0.05$; **Fig. S4 G**). The relative abundances of Proteobacteria and Bacteroides were decreased in the eMD and eHD group, whereas Firmicutes and Actinobacteria were increased (**Table S6** and **S7; Fig. S3A** and **B**). The above results showed that AAE could alter the diversity and composition of the gut microbiota *in vitro*, albeit with slight differences compared with *in vivo* observations.

We examined the effects of AAE treatment on different bacterial genera in faecal samples collected from MD rats. The relative abundances of *Blautia, Enterococcus, Faecalitalea*, *Lachnoclostridium*, *Parabacteroides*, *Phascolarctobacterium,* and *Roseburia* were increased (Fig. 3G). CCA (Fig. 3H) and permutation test (**Table S8**) were performed to examine the relationships between diabetes related factors and bacterial community composition. The plasma levels of 2h-PG ($r^2 = 0.42$, $p < 0.05$), TC ($r^2 = 0.58$, $p < 0.05$), (TG, $r^2 = 0.30$, $p < 0.05$), and ileum levels of TNFα ($r^2 = 0.42$, $p < 0.05$) were significantly correlated with the composition of the gut microbiota *in vivo* (Fig. 3H). Notably, the 2h-PG level was negatively correlated with the relative abundance of *Blautia, Enterococcus, Lachnoclostridium*, *Parabacteroides*, and *Roseburia* (Fig. 3H). These results suggest that these are potentially beneficial bacteria which can help to improve diabetes [6,46].

3.3. AAE enriched potentially beneficial bacteria and inhibited the growth of potentially harmful bacteria

Overall, the relative abundance of potentially beneficial bacteria increased with time, with the largest increase in MD rats (Fig. 4**A** and **B**). AAE also increased the abundance of certain SCFA-producing bacteria *in vitro*, with time-dependent increases in *Blautia*, *Lachnoclostridium,* and *Roseburia* (Fig. 4**C** and **D**). However, the optimal dose of AAE varied among the different bacterial genera, with the highest abundance of *Blautia* and *Lachnoclostridium* in the eMD group but the highest abundance of *Roseburia* in the eHD group (Fig. 4C).

Gas chromatography (GC)-MS analysis showed that concentrations of SCFAs such as acetic acid, propionic acid, and butyric acid were decreased in the DM group, while AAE could reverse these deficits in a dose-dependent manner, both *in vivo* and *in vitro* (**Fig. S5A** and **B**). CCA showed that SCFA concentrations were significantly correlated with the composition of the gut microbiota. Specifically, *Blautia* and *Enterococcus* were positively correlated with total SCFA and acetic acid concentrations, whereas *Roseburia*, *Parabacteroides*, and *Lachnoclostridium* were positively correlated with butyric acid concentration (**Fig. S5C** and **S5D**).

Blautia has previously been implicated in diabetes [47–53]. Many studies have shown negative correlations between *Blautia* and diabetes [49,48–53]. We further explored the anti-diabetic mechanisms of AAE by culturing a commercially available strain of *B. coccoides* in liquid medium containing varying levels of AAE for 24 h. AAE increased the relative abundance of *B. coccoides* in a dose-dependent manner at the concentrations $\geq$ 512 μg mL^{-1}, determined by optical density 600 nm (OD_{600nm}) measurements (Fig. 4I).

We also examined the effects of AAE on potentially harmful bacteria. CCA showed that *Facklamia*, *Oligella*, and *Klebsiella* were positively correlated with 2h-PG levels (Fig. 3H). Their relative abundances decreased with time after AAE treatment according to *in vivo* experiments (Fig. 4**E** and **F**), while *Klebsiella* also decreased with time after AAE incubation *in vitro* (Fig. 4**G** and **H**). Overall, AAE treatment, especially at a medium dose, increased the relative abundance of potentially beneficial bacteria and decreased potentially harmful bacteria, suggesting that these changes may be related to the alleviation of diabetes.

3.4. AAE restored endoplasmic reticulum, ribosomal, anti-oxidative stress protein levels and pancreatic islet cell function

We examined the effects of AAE treatment on the pancreas by analysing pancreatic protein expression in NM, DM, and AAE-treated rats using LC–MS in conjunction with the TMT labelling approach (**Fig. S6A**). Protein was extracted by in-gel digestion with trypsin, and

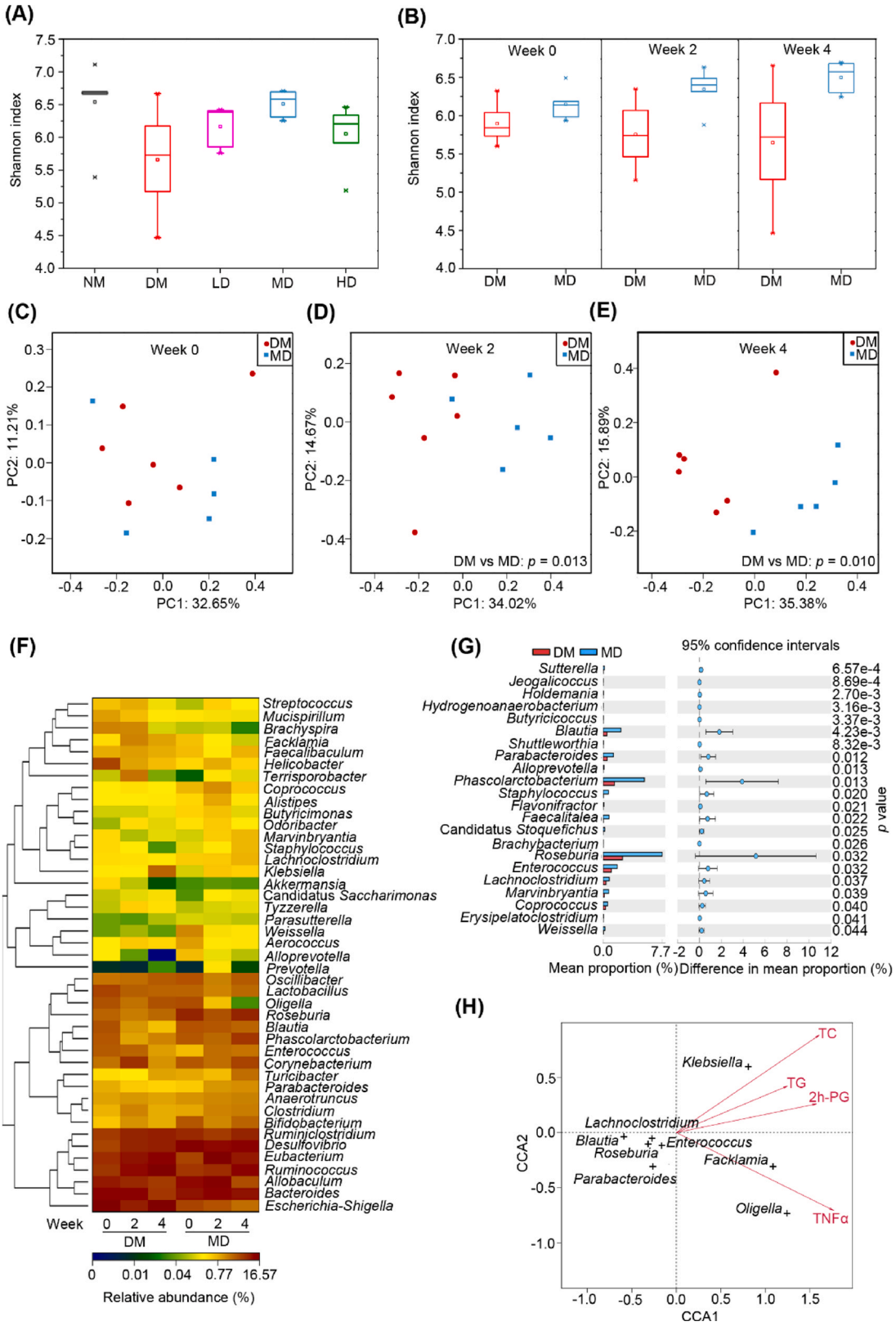

Fig. 3. AAE affected the diversity and composition of the gut microbiota in diabetic rats. (**A**) Shannon indices in NM, DM, and AAE-treated rats at week 4. Boxes show medians and interquartile ranges (IQRs); whiskers denote lowest and highest values within 1.5 times the IQRs from the first and third quartiles; outliers shown as individual points. (**B**) Shannon indices in MD rats at week 0, 2, and 4. Boxes, whiskers, and outliers denote values as described above. Principal co-ordinates analysis of microbial communities in MD and DM rats at weeks 0 (**C**), 2 (**D**), and 4 (*E*). PC1: principal component 1; PC2: principal component 2. (**F**) Heatmap analysis indicating relative abundances of dominant genera in MD and DM rats at weeks 0, 2, and 4. (**G**) STAMP analysis indicated genera that were significantly different between MD and DM rats at week 4. (**H**) CCA between gut microbiota community and related indices (2h-PG, TNFα in ileum, TC and TG in plasma).

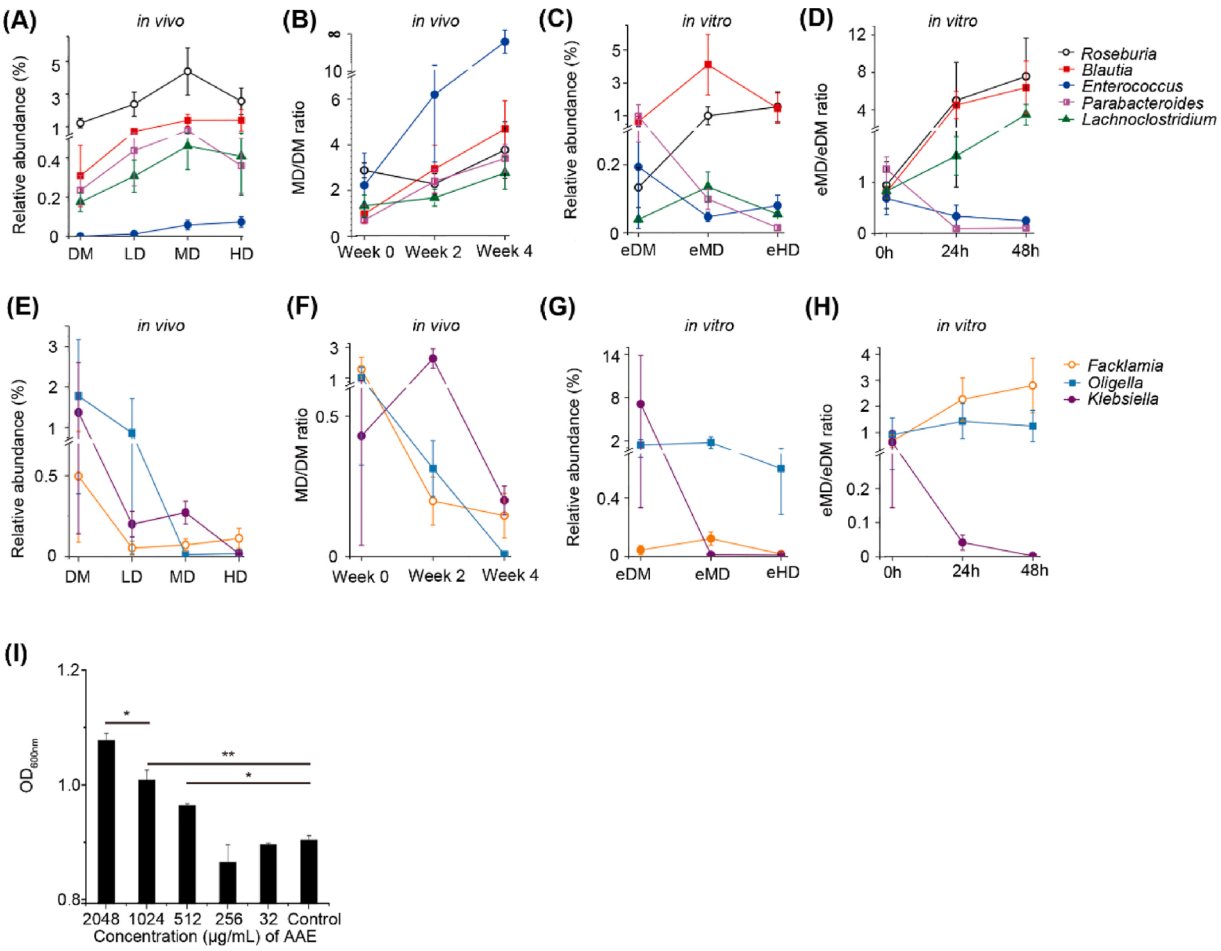

Fig. 4. AAE treatment promoted the proliferation of SCFA-producing bacteria and inhibited the growth of potentially harmful bacteria. Variations in relative abundances of potentially beneficial genera (rich in MD group and negatively correlated with 2h-PG, TC in plasma, TG in plasma, and TNFα in ileum) in DM and AAE-treated rats at week 4 *in vivo* (**A**), according to MD/DM ratio at week 0, 2, and 4 *in vivo* (**B**), in eDM, eMD, and eHD groups at 48 h *in vitro* (**C**), according to eMD/eDM ratio at 0, 24, and 48 h *in vitro* (**D**). Colours indicate same genera in **A–D**. Variations in relative abundances of potentially harmful genera (positively correlated with 2h-PG, TC in plasma, TG in plasma, and TNFα in ileum) in DM and AAE-treated rats at week 4 *in vivo* (*E*), according to MD/DM ratio at week 0, 2, and 4 *in vivo* (**F**), in eDM, eMD, and eHD groups at 48 h *in vitro* (**G**), and according to eMD/eDM ratio at weeks 0, 24, and 48 h *in vitro* (**H**). Colours indicate same genera in (*E*–**H**). (**I**) OD_{600nm} value for *B. coccoides* growth in various concentrations of AAE. $^{*}p < 0.05$, $^{**}p < 0.01$ by one-tailed *t*-test. Values shown as mean ± SEM.

sample purity was checked by sodium dodecyl sulfate-polyacrylamide gel electrophoresis (SDS-PAGE) (**Fig. S6B**). A total of 4439 proteins were identified, with a total FDR of 1% at both the peptide and protein levels. Among these, 4148 proteins were successfully quantified (Fig. 5A, **Table S9** and **S10**). The mean duplicates ratio was 1.01 and the standard deviation (SD) for technical replicates was 0.08. The results were comparable to those obtained using conventional TMT labelling [54] (**Fig. S6C**).

In our analysis, only proteins with two or more unique peptides, a quantification ratio ≥ 0.25 (3 × SD), and $p < 0.05$ were accepted as upregulated and downregulated proteins. A total of 841 proteins met these requirements, of which 381 (45.3 %) were upregulated (**Table S11**) and 460 (54.7 %) were downregulated (**Table S12**). We compared the protein expression patterns between the NM, DM, and AAE-treated groups (Fig. 5B). As the downregulated proteins were the major changed proteins, the DM downregulated proteins (DM *vs*. NM) and AAE-treated groups (AAE *vs*. DM) were showed in Fig. 5**C**. The downregulated proteins in DM group were partially restored in HD group after AAE administration (Fig. 5C). The GO analysis of down-regulated proteins indicated the normal biological functions were significantly injured in DM groups, including post-translation modification, extracellular exosome, transport, cytoplasmic vesicle, structural, and endoplasmic reticulum proteins (Fig. 5D).

We plotted the distribution of the $\log_2$ downregulated protein ratio for the DM *versus* the NM group and showed that the curve was negatively shifted (mean value -0.69), indicating that pancreatic proteins were mostly downregulated in the DM group (Fig. 6A). In contrast, the mean values for the LD *versus* the DM group, and for the MD *versus* the DM group were 0.01 and −0.05, respectively. These results suggest that low and medium doses of AAE had little or no significant effect on pancreatic protein expression. Heatmap analysis showed a similar trend with similar protein expression patterns in the LD and MD groups (Fig. 6B). Changes in protein expression patterns could only be detected in the HD group.

Protein-protein interaction analysis based on the STRING database showed that the proteins downregulated in the DM group were primarily RNA-processing, ribosomal, and cytoskeletal proteins and protein kinases secreted by acinar cells. These results suggest that pancreatic cell function was impaired in the DM group (Fig. 6C). Furthermore, most downregulated proteins were restored in the HD group (Fig. 6**D-G**). These results indicated that a high dose of AAE could trigger the repair or regeneration of pancreatic cells, possibly by restoring the function of pancreatic islet cells.

The anti-oxidant protein peroxiredoxin 4 (PRDX4) has several protein-protein interactions with proteins recovered in the HD group (Fig. 6H). Indeed, immunofluorescence microscopy of pancreatic

(A) Protein identification and quantification

Proteomics parameters	Results
Identified spectra	363006
PSM	34259
Identified peptides	24380
Identified proteins	4439
Quantified proteins	4148
Quantified proteins (unique peptides ≥2)	3110

(B) **Up-regulated and down-regulated proteins (compared with normal)**

	Differentially expressed proteins	Downregulated	Upregulated
DM	841	460	381
LD	1125	633	492
MD	1104	630	474
HD	796	463	333

Cutoff: ratio ≥ 3 SD (0.25); unique peptide≥2, p-value≤0.05.

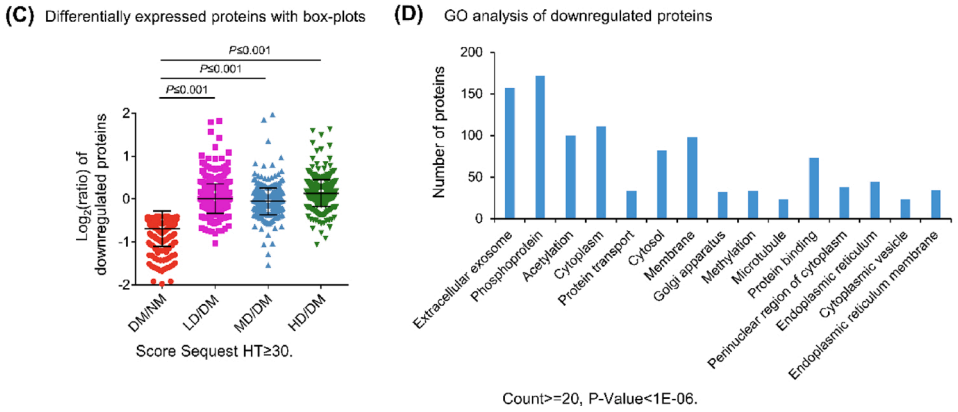

Fig. 5. The proteomic study flow chart and results analysis. (**A**) Summary of MS identification and quantitation. A total of 4148 proteins were quantified across all six groups. (**B**) Differentially expressed proteins among different groups. (**C**) Scatter plots of downregulated protein expression ratio for DM (*vs.* NM), LD (*vs.* DM), MD (*vs.* DM), and HD (*vs.* DM), respectively. (**D**) Biological function GO analysis of DM group downregulated proteins.

sections showed that PRDX4 was significantly downregulated in DM but upregulated in HD rats (Fig. 7**A and B**), as confirmed by haematoxylin-eosin (HE) and immunofluorescence staining (Fig. 7C). Specifically, pancreatic sections from DM rats showed atrophic islets, low islet count, enlarged cell vacuoles, islet nuclear pyknosis, increased nuclear heteromorphism, and signs of necrocytosis compared with NM rats. In contrast, sections from HD rats showed large improvements in islet morphology, some improvement in islet atrophy, increased islet count, and no signs of necrocytosis (Fig. 7C). These results support the efficacy of AAE treatment for promoting pancreatic repair and islet cell regeneration.

4. Discussion

TCMs have long been used to treat various diseases in China, but identifying the key components and molecular mechanisms underlying the treatments remains a challenge. After oral administration, the effects and mechanisms of multiple herbal constituents can be elucidated using classical molecular pharmacological methods [55]. Gut microbiota modulation might be a crucial aspect of the mechanism of the low oral bioavailability constituents. For example, Xu *et al.* demonstrated the involvement of gut microbiota modulation in the treatment effect of Gegen Qianlian Decoction on diabetes [9]. Notably, the components and metabolites of *A. asphodeloides* are with low oral bioavailability, and finding convincing evidence to support its mechanism of action thus poses a particular challenge [23–25]. The results of the current study revealed two previously unrecognized effects of AAE treatment: modulating the gut microbiota and triggering PRDX4 overexpression. Specifically, we demonstrated that unabsorbed components of AAE could help to regulate the gut microbiota and increase the abundance of beneficial bacteria such as *Blautia*, while the small proportion of absorbed components could promote cell regeneration in the pancreas and restore pancreatic islet cell function. This comprehensive investigation to reveal the mechanisms of AAE could thus be applied to the study of other TCMs.

Similar anti-diabetic effects (no significant differences) such as decrease of blood glucose, HOMA-IR, TC in plasma, *etc.* were observed in HD and MD group. However, high-dose and medium-dose AAE showed different pathways to alleviate diabetes. For examples, comparing to DM group, medium-dose AAE significantly changed the structure of gut bacterial community, while high-dose AAE didn't influence that significantly; high-dose AAE significant changed the relative abundance of pancreas function related proteins, but no significant changes were observed in MD group, which indicated medium-dose AAE was not adsorbed enough into the blood to alleviate diabetes through regulating the pancreas function. Specifically, the effective components of AAE in the MD group may be metabolites of flavonoids and saponins which mainly distributed in the gut. For example, norathyriol was not detected in plasma and mainly in faeces, especially in MD group. Previous study reported that oral administration of norathyriol protected mice from diet-induced obesity and insulin resistance [56], which indicated that norathyriol may improve the diabetes through modulating the gut microbiota. Differing from MD group, the effects of HD group are mainly attributed to the components which can be absorbed into the blood (such as Mangiferin), which could promote cell regeneration in the pancreas and restore pancreatic islet cell function.

There is growing evidence to suggest that diabetes is caused by an altered gut microbiota [11–13,57,58]. A high-fat diet can induce inflammation by changing the composition of the gut microbiota and increasing intestinal permeability *via* induction of Toll-like receptor 4, which accelerates the development of diabetes [13]. The gut microbiota suppresses insulin-mediated fat accumulation *via* the SCFA receptor GPR43 [57]. Qin et al. showed that patients with diabetes had a moderate degree of gut microbial dysbiosis, with a decrease in SCFA-producing bacteria and an increase in opportunistic pathogens [58]. The current *in vivo* and *in vitro* experiments showed that AAE enriched potentially beneficial bacteria. Importantly, co-incubation of AAE with faeces *in vitro* confirmed the changes in gut microbiota. However, the *in vitro* experiments showed some differences from the *in vivo* results. Maybe reproducing the anaerobic conditions that mimic the

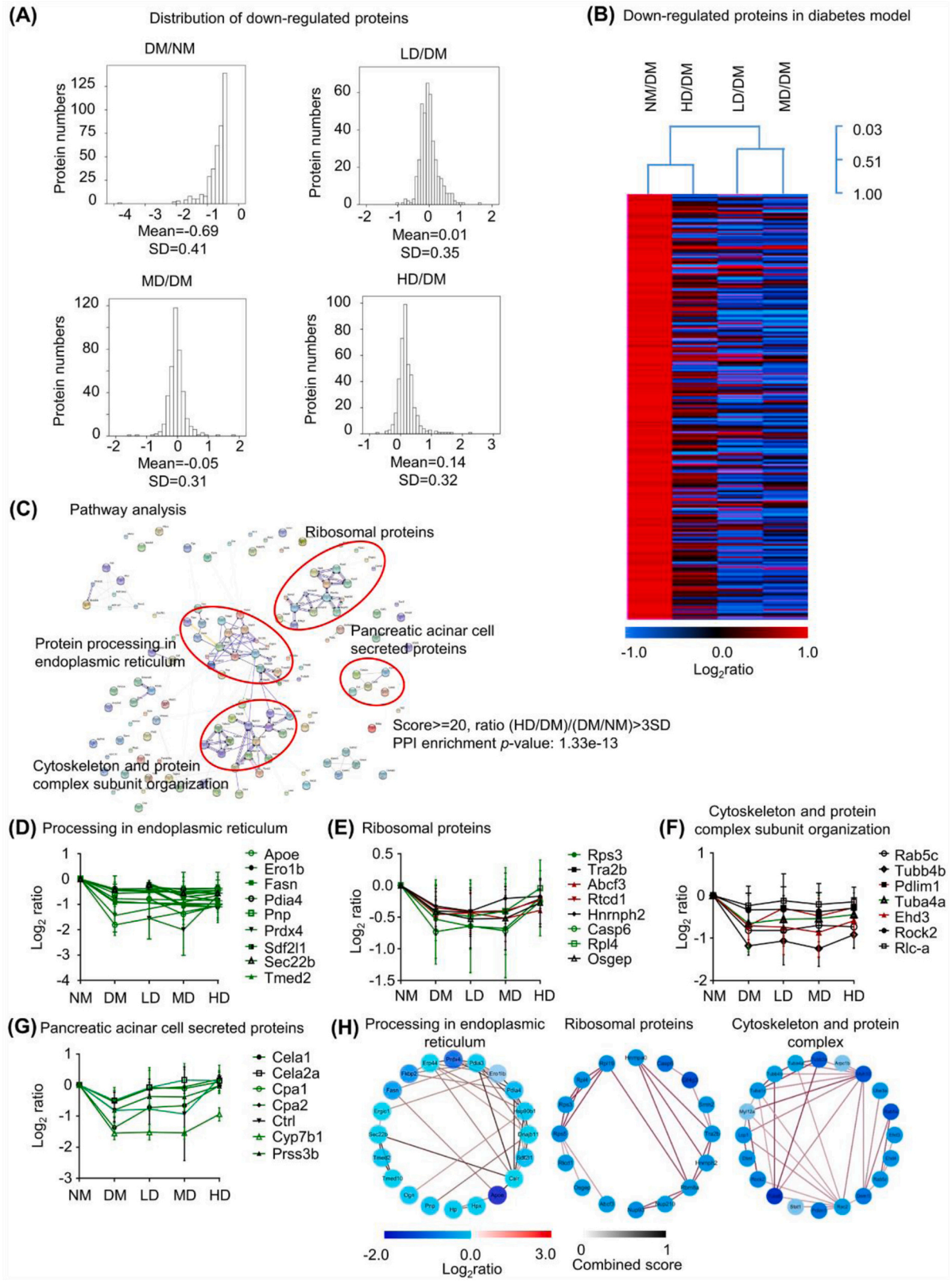

Fig. 6. Pancreas proteomics analysis after rats AAE administration. (**A**) Pancreatic proteins downregulated in diabetic rats with and without AAE. The $\log_2$ ratios of downregulated proteins were plotted in the different groups. The distribution curve for the DM group was negatively shifted compared with the control group, with a mean value of −0.69. The mean values were 0.01 for the LD compared with the DM group and −0.05 for the MD compared with the DM group. The distribution curve for the HD group was positively shifted compared with the DM group, with a mean value of 0.14. (**B**) Heatmap analysis of $\log_2$ ratio for downregulated proteins in four groups compared with the DM group. (**C**) Protein–protein interaction analysis of downregulated proteins using STRING. Areas surrounded by solid red lines represent functional protein clusters. Thick blue lines represent stronger associations. Relative peptide expression of major changed proteins for processing in endoplasmic reticulum (**D**), ribosomal proteins (*E*), cytoskeleton and protein complex subunit organization (**F**), and pancreatic acinar cell-secreted proteins (**G**). Protein network analysis showing highly connected proteins representative for each cluster in terms of downregulated proteins (**H**).

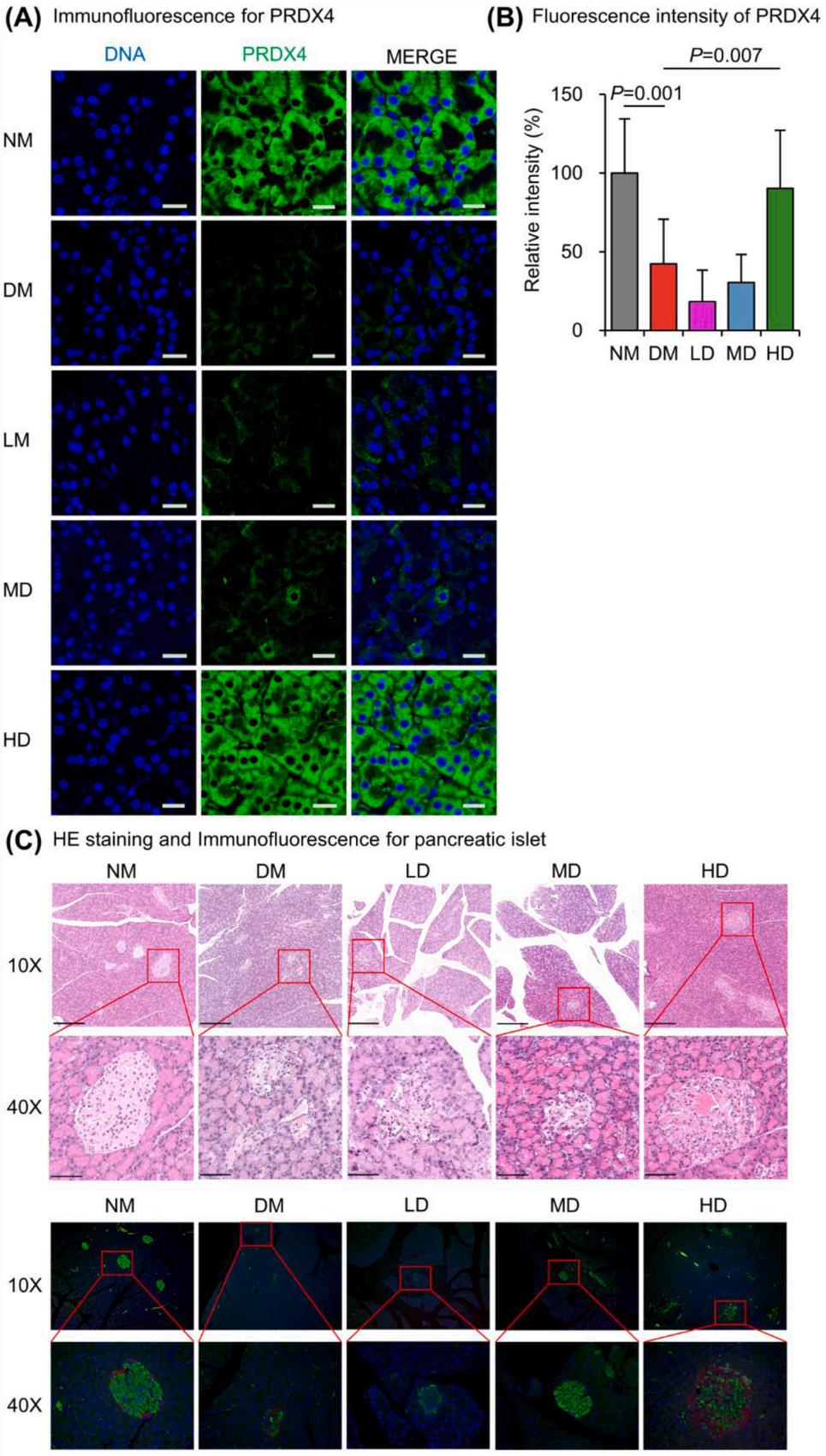

Fig. 7. The pancreatic islets of diabetic rats were recovered after AAE administration. (**A**) PRDX4 immunofluorescence in pathological sections of pancreatic islets from different groups. Scale bars =10 μm. (**B**) The intensity of PRDX4 was significantly downregulated in DM compared with control rats. PRDX4 was significantly upregulated after AAE administration compared with DM rats, to almost normal levels. (**C**) HE staining of pancreatic islets in pathological sections of pancreases in different groups (10×, scale bar =250 μm, 40×, Scale bars =50 μm). (**D**) Immunofluorescence staining of pancreatic islets in pathological sections of pancreases in different groups (10×, scale bars =250 μm, 40×, scale bar =50 μm).

gut environment and the effect of host factors cause these differences. AAE suppressed the relative abundance of Proteobacteria, consistent with another study showing that a mixture of *A. asphodeloides* and *Coptis chinensis* attenuated high-fat diet-induced colitis in mice [59]. AAE has also been shown to inhibit the growth of harmful bacteria such as *Facklamia*, *Oligella*, and *Klebsiella*, which all have pathogenic effects [60–63]. The inhibitory effects of *A. asphodeloides* on *Facklamia*, *Oligella*, and *Klebsiella* may thus help to maintain homeostasis and ameliorate diabetes.

Previous studies have shown that *Blautia* has positive implications for obesity and diabetes [49–53], consistent with the present study. Decaffeinated green and black tea polyphenols were shown to reduce weight gain and enrich *Blautia* in diet-induced obese mice [52]. Yang et al. demonstrated that xylooligosaccharide supplementation could enrich *Blautia* and improve glucose control in prediabetic adults [53]. Moreover, *Blautia* was also reportedly enriched by both metformin and a traditional Chinese herbal formula during the amelioration of blood glucose and lipid levels in a randomized clinical trial [51]. However, several studies have shown a possible association between *Blautia* and hyperglycemia [47,48]. De Filippis et al. [64] and Ferrocino et al. [50] recently found that different oligotypes of the same species showed different correlation patterns with metabolomic data. These authors attributed this conflict to different strains having different impacts on the host. In the current study, *Blautia* was significantly enriched in MD rats ($p < 0.01$) and was negatively correlated with 2h-PG levels, suggesting that *Blautia* are beneficial bacteria, at least in relation to diabetes. Indeed, *B. coccoides* (JCM 1395) proliferated in a dose-dependent manner after incubation with AAE. Overall, these results suggest that *Blautia* may be key to developing novel diabetes interventions.

The present proteomics analysis showed that HD AAE partially restored diabetes-induced protein downregulation. AAE also promoted pancreatic repair and triggered islet cell regeneration, indicating that high-dose AAE has certain therapeutic effects in rats. The concentrations of mangiferin, as one of the main components of AAE, were 5.40 and 3.65 times higher in the HD compared with the LD and MD groups, respectively, which suggests that mangiferin may be the effective component of AAE, as indicated previously [65].

PRDX4 is one of several antioxidant enzymes responsible for protecting organs during oxidative stress [66]. It is expressed in pancreatic islets, ductal epithelium, and small acinar cells. The current results showed that PRDX4 expression was downregulated in DM but restored in HD rats, suggesting that PRDX4 overexpression may trigger islet cell regeneration. PRDX4 overexpression might protect pancreatic β cells against streptozotocin-induced injury by suppressing the increased oxidative stress and inflammatory signalling activation [66].

5. Conclusions

Our study provides the first evidence that AAE alleviates diabetes through the modulation of gut microbiota and protein expression. The concentrations of main components and metabolites in faeces are several orders higher than those in plasma, which indicated that gut microbiota might play important roles in anti-diabetic effect of AAE. Microbiological studies show that unabsorbed components of AAE could help to prompt the growth of beneficial bacteria, such as *B. coccoides*, and inhibit disease-causing bacteria, while the small proportion of absorbed could promote cell regeneration in the pancreas and restore pancreatic islet cell function *via* PRDX4 overexpression. However, pathways and targets which alleviate diabetes through gut microbiota need to be further studied, and the diabetes–gut microbiota hypothesis thus needs to be verified in humans with lifestyle-induced diabetes. Our work elucidates the new thoughts of anti-diabetic mechanism of the *A. asphodeloides* possibly through combining regulation of gut microbiota and interactions between protein molecules using multi-omics. Furthermore, it could provide new solutions for verifying the mechanisms of low-oral-bioavailability natural products.

Author contributions

B. M., L. Y., P. X., and Y. D. designed the study, and discussed and summarized the anti-diabetic mechanism of *A. asphodeloides*. W. S. and B. Z. investigated the anti-diabetic effect of AAE on diabetic rats. Q. D., X. C., and J. Z. prepared and qualitatively analysed AAE. Q. D., X. S., and X. P. carried out qualitative analysis of faeces and plasma samples. D. Y. and T. Z. performed and analysed the *in vivo* and *in vitro* gut microbiota experiments. D. Y. conducted the bacterial growth experiments. W. X., T. Z., J. S., P. F., and P. X. performed the proteomics study using AAE-treated samples. P. F., P. C., and P. X. analysed the proteomics data. P. F., Q. D., and Y. H. performed validation experiments. D. Y., P. F., W. S., Q. D., and P. X. wrote the paper. All authors commented on the manuscript.

Funding

This work was supported by the National Natural Science Foundation of China (81773867,31870824), the National Science and Technology Major Project (2017ZX09301072, 2017YFA0505700, 2017YFC0906600, 2018ZX09711001-007-001), CAMS Innovation Fund for Medical Sciences (2016-I2M-2-002), the National Infrastructure of Microbial Resources (NIMR-2018-3), National Megaprojects for Key Infectious Diseases (2018ZX10302302001), and the CAMS Innovation Fund for Research Unit of Proteomics & Research and Development of New Drug (No.2019RU006).

Availability of data and materials

Raw reads were deposited in the NCBI Sequence Read Archive database under accession number SRP 144600.

Ethics approval and consent to participate

Male Wistar rats were purchased from the SPF Laboratory Animal Centre, Dalian Medical University, with permission number SCXK 2013–0003. All animals were maintained under standard laboratory conditions and according to the Guide for the Care and Use of Laboratory Animals (NIH).

Declaration of Competing Interest

The authors report no declarations of interest.

Acknowledgement

We thank Felix Cheung for critical reading and editing, laboratory members for their discussion and efforts, and Shuiming Wang and Haoyu Chen from Beijing BrightShines Technology Co., Ltd. for their help with immunohistochemistry analysis. We thank Susan Furness, PhD, from Liwen Bianji, Edanz Editing China (www.liwenbianji.cn/ac), for editing the English text of a draft of this manuscript.

Appendix A. Supplementary data

Supplementary material related to this article can be found, in the online version, at doi:https://doi.org/10.1016/j.biopha.2020.110954.

References

[1] A. Florencia, IDF Diabetes Atlas, eighth edition, International Diabetes Federation, 2017.
[2] S.E. Kahn, R.L. Hull, K.M. Utzschneider, Mechanisms linking obesity to insulin resistance and type 2 diabetes, Nature 444 (7121) (2006) 840.
[3] M. Stumvoll, B.J. Goldstein, T.W. van Haeften, Type 2 diabetes: principles of pathogenesis and therapy, Lancet 365 (9467) (2005) 1333–1346.

[4] G. Musso, R. Gambino, M. Cassader, Obesity, diabetes, and gut microbiota: the hygiene hypothesis expanded? Diabetes Care 33 (10) (2010) 2277.
[5] H. Yan, J. Lu, Y. Wang, W. Gu, X. Yang, J. Yu, Intake of total saponins and polysaccharides from Polygonatum kingianum affects the gut microbiota in diabetic rats, Phytomedicine 26 (2017) 45–54.
[6] L. Zhao, F. Zhang, X. Ding, G. Wu, Y.Y. Lam, X. Wang, H. Fu, X. Xue, C. Lu, J. Ma, Gut bacteria selectively promoted by dietary fibers alleviate type 2 diabetes, Science 359 (6380) (2018) 1151–1156.
[7] N. Arpaia, C. Campbell, X. Fan, S. Dikiy, J.V.D. Veeken, P. Deroos, H. Liu, J. R. Cross, K. Pfeffer, P.J. Coffer, Metabolites produced by commensal bacteria promote peripheral regulatory T cell generation, Nature 504 (7480) (2013) 451.
[8] A. Koh, A. Molinaro, M. Stahlman, M.T. Khan, C. Schmidt, L. Manneras-Holm, H. Wu, A. Carreras, H. Jeong, L.E. Olofsson, P.O. Bergh, V. Gerdes, A. Hartstra, M. de Brauw, R. Perkins, M. Nieuwdorp, G. Bergstrom, F. Backhed, Microbially produced imidazole propionate impairs insulin signaling through mTORC1, Cell 175 (4) (2018) 947–961, e17.
[9] J. Xu, F. Lian, L. Zhao, Y. Zhao, X. Chen, X. Zhang, Y. Guo, C. Zhang, Q. Zhou, Z. Xue, X. Pang, L. Zhao, X. Tong, Structural modulation of gut microbiota during alleviation of type 2 diabetes with a Chinese herbal formula, ISME J. 9 (3) (2015) 552–562.
[10] I. Kimura, K. Ozawa, D. Inoue, T. Imamura, K. Kimura, T. Maeda, K. Terasawa, D. Kashihara, K. Hirano, T. Tani, The gut microbiota suppresses insulin-mediated fat accumulation via the short-chain fatty acid receptor GPR43, Nat. Commun. 4 (2013) 1829.
[11] N. Tai, F.S. Wong, L. Wen, The role of gut microbiota in the development of type 1, type 2 diabetes mellitus and obesity, Rev. Endocr. Metab. Dis. 16 (1) (2015) 55–65.
[12] P.D. Cani, M. Osto, L. Geurts, A. Everard, Involvement of gut microbiota in the development of low-grade inflammation and type 2 diabetes associated with obesity, Gut Microbes 3 (4) (2012) 279–288.
[13] K.A. Kim, W. Gu, I.A. Lee, E.H. Joh, D.H. Kim, High fat diet-induced gut microbiota exacerbates inflammation and obesity in mice via the TLR4 signaling pathway, PLoS One 7 (10) (2012), e47713.
[14] J.C. Chan, Y. Zhang, G. Ning, Diabetes in China: a societal solution for a personal challenge, Lancet Diabetes Endo. 2 (12) (2014) 969–979.
[15] W. Xie, Y. Zhao, Y. Zhang, Traditional chinese medicines in treatment of patients with type 2 diabetes mellitus, Evidence-Based Complementray and Alternative Medicine (2011) (2011) 726723 (2011-01-27) 2011(1741-427X).
[16] Y. Wang, Y. Dan, D. Yang, Y. Hu, L. Zhang, C. Zhang, H. Zhu, Z. Cui, M. Li, Y. Liu, The genus Anemarrhena Bunge: a review on ethnopharmacology, phytochemistry and pharmacology, J. Ethnopharmacol. 153 (1) (2014) 42–60.
[17] F. Cai, L. Sun, S. Gao, Y. Yang, Q. Yang, W. Chen, A rapid and sensitive liquid chromatography–tandem mass spectrometric method for the determination of timosaponin B-II in blood plasma and a study of the pharmacokinetics of saponin in the rat, J. Pharmaceut. Biomed. 48 (5) (2008) 1411–1416.
[18] D. Han, C. Chen, C. Zhang, Y. Zhang, X. Tang, Determination of mangiferin in rat plasma by liquid–liquid extraction with UPLC–MS/MS, J. Pharmaceut. Biomed. 51 (1) (2010) 260–263.
[19] X. Tian, Z. Xu, Z. Li, Y. Ma, S. Lian, X. Guo, P. Hu, Y. Gao, C. Huang, Pharmacokinetics of mangiferin and its metabolite—norathyriol, Part 2: influence of UGT, CYP450, P-gp, and enterobacteria and the potential interaction in Rhizoma Anemarrhenae decoction with timosaponin B2 as the major contributor, BioFactors 42 (5) (2016) 545–555.
[20] P. Apontes, Z. Liu, K. Su, O. Benard, D.Y. Youn, X. Li, W. Li, R.H. Mirza, C.C. Bastie, L.A. Jelicks, Mangiferin Stimulates Carbohydrate Oxidation and Protects Against High Fat Diet Induced Metabolic Disorders, 2014.
[21] Fei Cai, Lianna Sun, Shouhong Gao, Yang, A rapid and sensitive liquid chromatography–tandem mass spectrometric method for the determination of timosaponin B-II in blood plasma and a study of the pharmacokinetics of saponin in the rat, J. Pharm. Biomed. Anal. (2008).
[22] Y. Tang, Z. Sun, M. Fan, Z. Li, C. Huang, Anti-diabetic effects of TongGuanWan, a Chinese traditional herbal formula, in C57BL/KsJ-db/db mice, Planta Med. 78 (01) (2012) 18–23.
[23] B.F. Bitner, J.D. Ray, K.B. Kener, J.A. Herring, J.A. Tueller, D.K. Johnson, C. M. Tellez Freitas, D.W. Fausnacht, M.E. Allen, A.H. Thomson, K.S. Weber, R. P. McMillan, M.W. Hulver, D.A. Brown, J.S. Tessem, A.P. Neilson, Common gut microbial metabolites of dietary flavonoids exert potent protective activities in beta-cells and skeletal muscle cells, J. Nutr. Biochem. 62 (2018) 95–107.
[24] J.K. Bird, D. Raederstorff, P. Weber, R.E. Steinert, Cardiovascular and antiobesity effects of resveratrol mediated through the gut microbiota, Adv. Nutr. 8 (6) (2017) 839–849.
[25] C.A. Edwards, J. Havlik, W. Cong, W. Mullen, T. Preston, D.J. Morrison, E. Combet, Polyphenols and health: Interactions between fibre, plant polyphenols and the gut microbiota, Nutr. Bull. 42 (4) (2017) 356–360.
[26] M. Samuel, S.B. Karen, Modified glucose oxidase method for determination of glucose in whole blood, Clin. Chem. (3) (1973) 308–311.
[27] L.P. Kang, J. Zhang, Y. Cong, B. Li, C.Q. Xiong, Y. Zhao, D.W. Tan, H.S. Yu, Z.Y. Yu, Y.W. Cong, Steroidal glycosides from the rhizomes of Anemarrhena asphodeloides and their antiplatelet aggregation activity, Planta Med. 78 (06) (2012) 611–616.
[28] S.A. Huws, J.E. Edwards, E.J. Kim, N.D. Scollan, Specificity and sensitivity of eubacterial primers utilized for molecular profiling of bacteria within complex microbial ecosystems, J. Microbiol. Methods 70 (3) (2007) 565–569.
[29] J.G. Caporaso, C.L. Lauber, W.A. Walters, D. Berg-Lyons, J. Huntley, N. Fierer, S. M. Owens, J. Betley, L. Fraser, M. Bauer, N. Gormley, J.A. Gilbert, G. Smith, R. Knight, Ultra-high-throughput microbial community analysis on the Illumina HiSeq and MiSeq platforms, ISME J. 6 (8) (2012) 1621–1624.
[30] Q. Wang, G.M. Garrity, J.M. Tiedje, J.R. Cole, Naive Bayesian classifier for rapid assignment of rRNA sequences into the new bacterial taxonomy, Appl. Environ. Microbiol. 73 (16) (2007) 5261–5267.
[31] K.R. Amato, C.J. Yeoman, A. Kent, N. Righini, F. Carbonero, A. Estrada, H. R. Gaskins, R.M. Stumpf, S. Yildirim, M. Torralba, M. Gillis, B.A. Wilson, K. E. Nelson, B.A. White, S.R. Leigh, Habitat degradation impacts black howler monkey (Alouatta pigra) gastrointestinal microbiomes, ISME J. 7 (7) (2013) 1344–1353.
[32] X. Mei, X. Zhang, Z. Wang, Z. Gao, G. Liu, H. Hu, L. Zou, X. Li, Insulin Sensitivity-Enhancing Activity of Phlorizin is associated with Lipopolysaccharides decrease and Gut Microbiota Changes in obese and type 2 diabetes (db/db) Mice, J. Agric. Food Chem. 64 (40) (2016) 7502.
[33] Y. Zhang, Y. Li, Y. Zhang, Z. Wang, M. Zhao, N. Su, T. Zhang, L. Chen, W. Wei, J. Luo, Quantitative proteomics reveals membrane protein-mediated hypersaline sensitivity and adaptation in halophilic Nocardiopsis xinjiangensis, J. Proteome Res. 15 (1) (2016) 68.
[34] Pichler Peter, Köcher Thomas, Holzmann Johann, Mazanek Michael, Taus Thomas, Peptide labeling with isobaric tags yields higher identification rates using iTRAQ 4-Plex compared to TMT 6-Plex and iTRAQ 8-Plex on LTQ orbitrap, Anal. Chem. (2010).
[35] K.A. Welle, T. Zhang, J.R. Hryhorenko, S. Shen, J. Qu, S. Ghaemmaghami, Time-resolved analysis of proteome dynamics by tandem mass tags and stable isotope labeling in cell culture (TMT-SILAC) hyperplexing, Mol. Cell Proteomics 15 (12) (2016) 3551.
[36] G. Dennis, B.T. Sherman, D.A. Hosack, J. Yang, W. Gao, H.C. Lane, R.A. Lempicki, DAVID: Database for Annotation, Visualization, and Integrated Discovery, Genome Biol. 4 (5) (2003) P3.
[37] M. Kanehisa, M. Furumichi, T. Mao, Y. Sato, K. Morishima, KEGG: new perspectives on genomes, pathways, diseases and drugs, Nucleic Acids Res, 45 (Database issue) (2017) D353–D361.
[38] M. Kanehisa, Y. Sato, M. Kawashima, M. Furumichi, M. Tanabe, KEGG as a reference resource for gene and protein annotation, Nucleic Acids Res. 44 (Database issue) (2016) D457–D462.
[39] D. Szklarczyk, A. Franceschini, S. Wyder, K. Forslund, D. Heller, J. Huertacepas, M. Simonovic, A. Roth, A. Santos, K.P. Tsafou, STRING v10: protein–protein interaction networks, integrated over the tree of life, Nucleic Acids Res, 43 (Database issue) (2015) D447.
[40] R.C. Team, R: a Language and Environment for Statistical Computing, Available at: , R Foundation for Statistical Computing, Vienna, Austria, 2018 http://www.r-project.org.
[41] D.H. Parks, G.W. Tyson, P. Hugenholtz, R.G. Beiko, STAMP: statistical analysis of taxonomic and functional profiles, Bioinformatics 30 (21) (2014) 3123.
[42] Y. Zhao, L. Kang, H. Yu, J. Zhang, C. Xiong, X. Pang, Y. Gao, C. Liu, B. Ma, Structure characterization and identification of steroidal saponins from the rhizomes of Anemarrhena asphodeloides by ultra performance liquid chromatography and hybrid quadrupole time-of-flight mass spectrometry, Int. J. Mass Spectrom.s 341–342 (5) (2013) 7–17.
[43] S.H. Nian, H.J. Li, E.H. Liu, P. Li, Comparison of α-glucosidase inhibitory effect and bioactive constituents of Anemarrhenae Rhizoma and Fibrous Roots, J. Pharm. Biomed. Anal. 145 (2017) 195–202.
[44] D. Li, R. Xue, Z. Li, M. Chen, W. Jiang, C. Huang, In vivo metabolism study of timosaponin BIII in rat using HPLC-QTOF-MS/MS, Chromatographia 77 (11–12) (2014) 853–858.
[45] L. Su-Min, J. Jin-Ju, K. Geum-Dan, K. Kyung-Ah, C. Hyun-Sik, K. Dong-Hyun, Timosaponin AIII and its metabolite sarsasapogenin ameliorate colitis in mice by inhibiting NF-κB and MAPK activation and restoring Th17/Treg cell balance, Int. Immunopharmacol. 25 (2) (2015) 493–503.
[46] M. Remely, E. Aumueller, C. Merold, S. Dworzak, B. Hippe, J. Zanner, A. Pointner, H. Brath, A.G. Haslberger, Effects of short chain fatty acid producing bacteria on epigenetic regulation of FFAR3 in type 2 diabetes and obesity, Gene 537 (1) (2014) 85–92.
[47] D.A. Kashtanova, O.N. Tkacheva, E.N. Doudinskaya, I.D. Strazhesko, Y. V. Kotovskaya, A.S. Popenko, A.V. Tyakht, D.G. Alexeev, Gut microbiota in patients with different metabolic statuses: moscow study, Microorganisms 6 (4) (2018) 98.
[48] I. Leiva-Gea, L. Sanchez-Alcoholado, B. Martin-Tejedor, D. Castellano-Castillo, I. Moreno-Indias, A. Urda-Cardona, F.J. Tinahones, J.C. Fernandez-Garcia, M. I. Queipo-Ortuno, Gut microbiota differs in composition and functionality between children with type 1 diabetes and MODY2 and healthy control subjects: a case-control study, Diabetes Care 41 (11) (2018) 2385–2395.
[49] M. Murri, I. Leiva, J.M. Gomez-Zumaquero, F.J. Tinahones, F. Cardona, F. Soriguer, M.I. Queipo-Ortuno, Gut microbiota in children with type 1 diabetes differs from that in healthy children: a case-control study, BMC Med. 11 (2013) 46.
[50] I. Ferrocino, V. Ponzo, R. Gambino, A. Zarovska, F. Leone, C. Monzeglio, I. Goitre, R. Rosato, A. Romano, G. Grassi, F. Broglio, M. Cassader, L. Cocolin, S. Bo, Changes in the gut microbiota composition during pregnancy in patients with gestational diabetes mellitus (GDM), Sci. Rep. 8 (1) (2018) 12216.
[51] X. Tong, J. Xu, F. Lian, X. Yu, Y. Zhao, L. Xu, M. Zhang, X. Zhao, J. Shen, S. Wu, X. Pang, J. Tian, C. Zhang, Q. Zhou, L. Wang, B. Pang, F. Chen, Z. Peng, J. Wang, Z. Zhen, C. Fang, M. Li, L. Chen, L. Zhao, Structural alteration of gut microbiota during the amelioration of human type 2 diabetes with hyperlipidemia by metformin and a traditional chinese herbal formula: a multicenter, randomized, open label clinical trial, MBio 9 (3) (2018) e02392–17.
[52] S.M. Henning, J. Yang, M. Hsu, R.P. Lee, E.M. Grojean, A. Ly, C.H. Tseng, D. Heber, Z. Li, Decaffeinated green and black tea polyphenols decrease weight gain and alter

microbiome populations and function in diet-induced obese mice, Eur. J. Nutr. 57 (8) (2018) 2759–2769.
[53] Y. Jieping, P.H. Summanen, S.M. Henning, H. Mark, L. Heiman, H. Jianjun, T. Chi-Hong, S.E. Dowd, S.M. Finegold, H. David, Xylooligosaccharide supplementation alters gut bacteria in both healthy and prediabetic adults: a pilot study, Front. Physiol. 6 (6) (2015) 216.
[54] Z. Wang, J. Ma, C. Miyoshi, Y. Li, M. Sato, Y. Ogawa, T. Lou, C. Ma, X. Gao, C. Lee, Quantitative phosphoproteomic analysis of the molecular substrates of sleep need, Nature 558 (2018) 435–439.
[55] L. Wang, G. Zhou, P. Liu, J.H. Song, Y. Liang, X.J. Yan, F. Xu, B.S. Wang, J.H. Mao, Z. Shen, Dissection of mechanisms of Chinese medicinal formula Realgar-Indigo naturalis as an effective treatment for promyelocytic leukemia, P. Natl, Acad. Sci. USA 105 (12) (2008) 4826–4831.
[56] Zen Ke, Zhang Yujing, Ding Hanying, Xu Chen, Zhang Yan, Norathyriol reverses obesity- and high-fat-diet-induced insulin resistance in mice through inhibition of PTP1B, Organ of the European Association for the Study of Diabetes (2014).
[57] I. Kimura, K. Ozawa, D. Inoue, T. Imamura, K. Kimura, T. Maeda, K. Terasawa, D. Kashihara, K. Hirano, T. Tani, T. Takahashi, S. Miyauchi, G. Shioi, H. Inoue, G. Tsujimoto, The gut microbiota suppresses insulin-mediated fat accumulation via the short-chain fatty acid receptor GPR43, Nat. Commun. 4 (2013) 1829.
[58] J. Qin, Y. Li, Z. Cai, S. Li, J. Zhu, F. Zhang, S. Liang, W. Zhang, Y. Guan, D. Shen, A metagenome-wide association study of gut microbiota in type 2 diabetes, Nature 490 (7418) (2012) 55.
[59] S.M. Lim, H.S. Choi, J.J. Jeong, S.W. Han, D.H. Kim, The rhizome mixture of *Anemarrhena asphodeloides* and *Coptis chinensis* Attenuates mesalazine-resistant colitis in mice, Evid.-Based Compl. Alt. 2016 (5895184) (2016) 1–9.
[60] R. Podschun, U. Ullmann, Klebsiella spp. As nosocomial pathogens: epidemiology, taxonomy, typing methods, and pathogenicity factors, Clin. Microbiol. Rev. 11 (4) (1998) 589–603.
[61] E. Rahmati, V. Martin, D. Wong, F. Sattler, J. Petterson, P. Ward, S.M. Butler-Wu, R.C. She, Facklamia species as an underrecognized pathogen, Open Forum Infect. Di. 4 (1) (2017) ofw272.
[62] H. Yamaguchi, Y. Yamaguchi, Y. Hadano, K. Hayashi, C. Nagahara, T. Muratani, K. Ohkusu, The first case report of emphysematous pyelonephritis and bacteremia due to Oligella urethralis, Int. J. Med. Microbiol. 307 (3) (2017) 151–153.
[63] H. Li, T. Qi, Z.S. Huang, Y. Ying, Y. Zhang, B. Wang, L. Ye, B. Zhang, D.L. Chen, J. Chen, Relationship between gut microbiota and type 2 diabetic erectile dysfunction in Sprague-Dawley rats, J. Huazhong Univ. Sci. Technol. Med. Sci. 37 (4) (2017) 523–530.
[64] F. De Filippis, N. Pellegrini, L. Laghi, M. Gobbetti, D. Ercolini, Unusual sub-genus associations of faecal Prevotella and Bacteroides with specific dietary patterns, Microbiome 4 (1) (2016) 57.
[65] H.L. Wang, C.Y. Li, B. Zhang, Y.D. Liu, B.M. Lu, Z. Shi, N. An, L.K. Zhao, J.J. Zhang, J.K. Bao, Mangiferin facilitates islet regeneration and β-cell proliferation through upregulation of cell cycle and β-cell regeneration regulators, Int. J. Mol. Sci. 15 (5) (2014) 9016.
[66] S. Yamada, Y. Ding, Y. Sasaguri, Peroxiredoxin 4: critical roles in inflammatory diseases, J. UOEH 34 (1) (2012) 27–39.